

## Enhancing the Removal of Organic Pollutant-Methylene Blue- by a Moroccan Natural Clay

M. EL Alouani\*, S. Alehyen, M. Zerzouri, M. EL Achouri, M. Taibi

Laboratoire de Physico-chimie des Matériaux Inorganiques et Organiques (LPCMIO), Centre des Sciences des Matériaux (CSM). Ecole Normale Supérieure BP : 5118. Takaddoum -Rabat-Morocco Mohammed V University in Rabat,

### Abstract

In this study, the removal of a cationic dye namely, methylene blue (MB) by natural clay (NC) from aqueous solution was investigated. The morphology, structure and surface state of NC were characterized using X-Ray Diffraction (XRD), X-Ray Fluorescence (XRF), Fourier Transform Infrared Spectroscopy (FTIR), Differential Scanning Calorimetry (DSC), Scanning Electron Microscopy (SEM) and Optical Microscope, respectively. Affecting factors solution pH, dye concentration, contact time and temperature were investigated. The maximum removal was obtained at basic pH. The experimental equilibrium data were examined using Langmuir, Freundlich, Temkin and Dubinin–Radushkevich. The equilibrium data for cationic dye adsorption was fitted to the Langmuir, and the maximum adsorption capacity of natural clay for MB was up to 25 mg.g<sup>-1</sup>. The adsorption kinetic dye was analyzed using pseudo-first order, pseudo-second order, Elovish and the intraparticle diffusion model. The kinetic data of cationic dye could be better described by the pseudo second-order model. The thermodynamic parameters such as the change in free energy ( $\Delta G^\circ$ ), enthalpy ( $\Delta H^\circ$ ) and entropy ( $\Delta S^\circ$ ) of adsorption were determined. These values show that the adsorption was exothermic and spontaneous.

\* Corresponding author:

[ma.elalouani@gmail.com](mailto:ma.elalouani@gmail.com)

Received 19 Oct 2018,

Revised April 2019,

Accepted 04 Aug 2019

**Keywords:** Natural clay; Adsorption model; Kinetics; Thermodynamics; Cationic dye

## 1. Introduction

Dyes are important compound commonly used in various industries such as textile, paper, leather and plastic manufacture [1]. The discharge of dye-containing effluent without proper treatment into water bodies causes both environmental and public health risks [2]. Among the textile dyes most used in industry, methylene blue (MB) or basic blue 9, it is a water-soluble cationic dye, MB is considered to be a very toxic dye, it can reveal very harmful effects on living things such as difficulties in breathing, vomiting, diarrhea and nausea [3], and In addition, textile dyes can affect plants that live in aquatic environments because they reduce the transmission of sunlight through water. Therefore it is very important to confirm the water quality, since even just 1.0 mg/L of dye concentration in drinking water can impart a significant color, making it unfit for human consumption [4]. Therefore, it is necessary to reduce dyes concentration in wastewater. Nowadays, various technologies are available for the removal of toxic substances from wastewaters, such as biological treatment [5], biochemical methods [6], membrane separation [7], ion-exchange[8], ultrafiltration[9], electrochemical processes [10], coagulation/flocculation [11], adsorption [12] and other processes. Adsorption process has proven to be highly effective in the remediation of dyes from wastewater, especially if the adsorbent is inexpensive and readily available [13]. In literature, many adsorbents have been investigated for the removal of methylene blue from aqueous solutions, such, as Kaolinite[14], Illite[15], Zeolitic[16], Fly ash[17], Palm [18]. The use of natural materials is a promising alternative due to their relative [19]. The focus of the present study was to determine the adsorption capacity of the MB using NC. Adsorption studies were carried out under various parameters such as pH, contact time, initial dye concentration and temperature. The equilibrium data were analyzed using Langmuir, Freundlich, Temkin isotherm and Dubinin–Radushkevich models. Kinetic models data were tested by pseudo-first-order, pseudo second-order, elovich and intra-particle diffusion kinetic models. The thermodynamics of the adsorption was also evaluated.

## 2. Materials and methods

### 2.1. Adsorbent, adsorbate and materials

The natural clay ( NC) used in this work was collected from Nador region in Morocco, It was crushed, sieved through sieve to obtain lower fractions (<120  $\mu\text{m}$ ), then dried in an oven at 105°C during 24 hour and stored in sealed containers prior to use. The adsorbent was characterized using XRD (Xpert Pro model), FTIR (VERTEX 70FTIR), Image of NC was characterized by a detector type (SUTW-Sapphire, Resolution: 230.89, Lsec: 111), Optical microscope (Microscope leica DVM5000 Zoom: 350X) and DSC was conducted at heating rate of 10°C/min from 25°C to 750°C in argon atmosphere by using a SETARAM 121 apparatus. Methylene Blue (MB) is a cationic dye of formula  $\text{C}_{16}\text{H}_{18}\text{ClN}_3\text{S}$ , with  $319.852 \pm 0.022$  g/mol as a molecular weight and  $\lambda_{\text{max}}$ : 665 nm. Its structure is shown in Figure 1. Methylene Blue was used as principal adsorbate without further purification. The MB used in the work was the analytical grade on (Aldrich Chemistry, Germany).

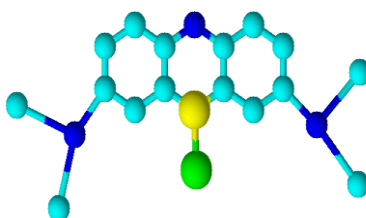


**Figure 1:** The Chemical structure of Methylene Blue (MB)

## 2.2. Adsorption tests

The adsorption experiments were performed by batch process. To optimize the process of removing MB, different parameters such as: pH medium, contact time, the initial concentration of MB and the temperature of the solution have been taken into consideration. The influence of the initial pH was studied at for 1h a range of pH value from 2 to 14. Dye solution pH was adjusted using 0.1M NaOH and 0.1M HCl solutions and measured using a Meter Lab, pH M 210 meter. The effect of contact time on the adsorption of dye from solution was investigated at different time intervals in the range of 10- 180 min to analyze the adsorption kinetic of MB by NC. The effect of initial dye concentration from 10 to 40 mg/L was conducted to determine the adsorption capacity of the NC. The influence of temperature on the adsorption onto NC was carried out at 3 different temperatures ranging from 20 to 70°C to evaluate the natural of adsorption. After each completed absorption test, the sample was separated by centrifuge at 2500 rpm for 10 min to separate the solid phase from the liquid phase. The residual dye concentrations of each solution were determined by JASCO V-630 UV/VIS spectrophotometer. The adsorption capacity of MB at equilibrium (mg/g) was calculated using by Eq (1):

$$Q_e = \frac{(C_0 - C_e)}{m} V \quad (1)$$

Where  $C_0$  and  $C_e$  are the initial and the equilibrium concentration of dye (mg/L), respectively,  $m$  is the amount of adsorbent (g) and  $V$  is the volume of solution (L).

The absorbance value obtained in each case was then used to calculate the % removal of the dye on NC [20], by using the following equation, Eq. (2):

$$\% \text{ Removal} = \frac{(A_i - A_t)}{A_i} \times 100 \quad (2)$$

Where  $A_i$  and  $A_t$  are the initial and any time  $t$  absorbance values, respectively.

## 2.3. Characterization of adsorbent

### *X-ray diffraction and X-ray fluorescence analysis*

The identification of NC is conducted by XRD patterns. As show in Figure 2. The results of XRD data obtained that the sample contained of montmorillonite (M), kaolinite (K) and quartz (Q). The significant peaks observed on the XRD patterns of the sample indicated that this NC is the sample rich in montmorillonite. The composition confirmed by X-ray fluorescence data Table 1 showing the presence of silica and alumina as major constituents, with traces of sodium, potassium, calcium, magnesium, iron, and titanium oxides in the form of impurities.

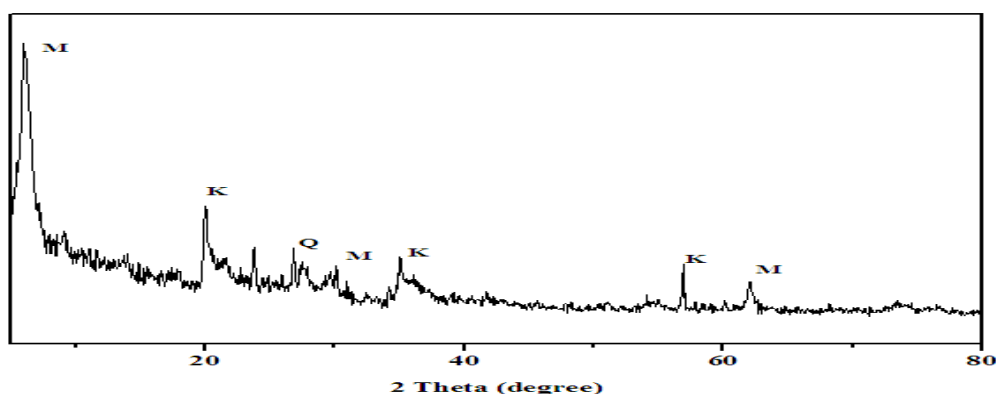


**Figure 2:** X-ray diffraction pattern of NC (M: Montmorillonite, K: Kaolin, Q: Quartz)

**Table 1:** Chemical composition of NC in this study by XRF

Composition	SiO <sub>2</sub>	Al <sub>2</sub> O <sub>3</sub>	Fe <sub>2</sub> O <sub>3</sub>	MgO	CaO	Na <sub>2</sub> O	K <sub>2</sub> O	TiO <sub>2</sub>	P <sub>2</sub> O <sub>5</sub>	SO <sub>3</sub>	Loss ignition
Percentage (wt%)	57.7	18.8	3.03	4.87	1.82	2.14	1.35	0.481	0.189	0.204	8.9

**FTIR spectra analysis**

The FTIR spectrum of NC before and after impregnation was presented in Figure 3. The adsorption band at 3616 cm<sup>-1</sup> was due to stretching vibration of structural –OH groups of clay. The peaks at 3556 and 1616 cm<sup>-1</sup> were attributed to the H<sub>2</sub>O stretching vibration and bending vibration, respectively. The band at 993 cm<sup>-1</sup> is due to the Si–O bending vibrations. The sharp peak at 769 cm<sup>-1</sup> was confirmed the quartz in NC [21]. The bands at 534 and 454 cm<sup>-1</sup> were due to Al–O–Si and Si–O–Si bending vibrations, respectively. The band corresponding to Al–Al–OH was observed at 993 cm<sup>-1</sup>[22]. After adsorption, characteristic bands at 1142, 1120 and 1086 cm<sup>-1</sup> were observed. The news bands at 1142 and 1120 cm<sup>-1</sup> duo the stretching heterocyclic of C–N [23]. The band at 1086 cm<sup>-1</sup> assigned stretching asymmetric vibration of C–S–C [24–27]. The results indicated that the reduction the peaks of NC and appearance of new peaks after adsorption occurred by the retention of MB molecules.

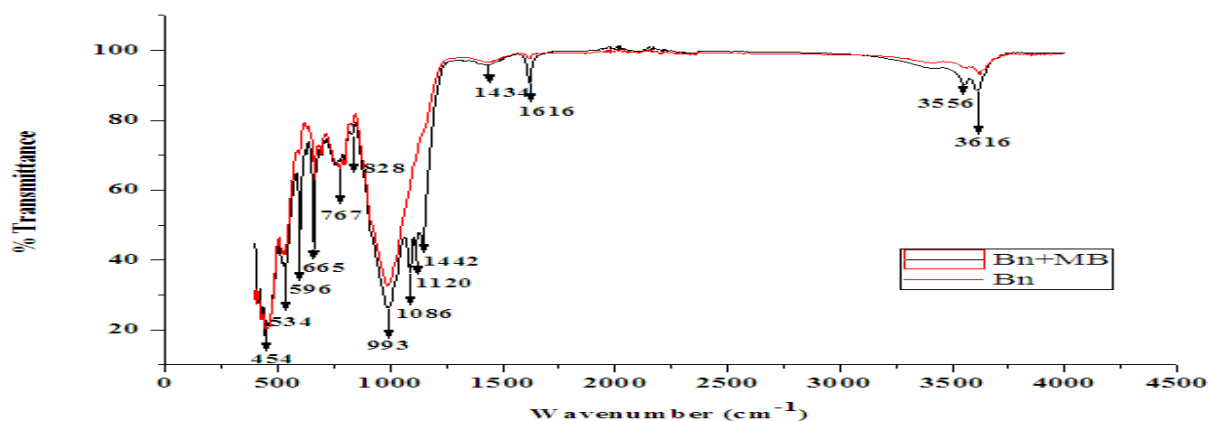
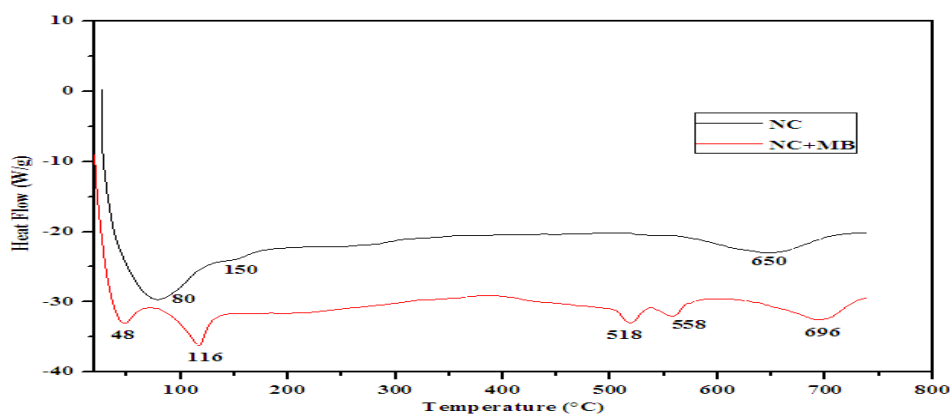
**Figure 3:** FTIR spectra of NC before (a) and after (b) adsorption of MB**Thermal analysis (DSC)**

Figure 4 shows the DSC curves of natural clay before and after adsorption of MB. The endothermic peak of NC adsorbent at 80°C was assigned to the evaporation of adsorbed water. The mass loss at 160 and 300°C is related to escape of interlayer water at different structural positions in NC. The dehydroxylation of NC and the decomposition of calcite intensively occur at 490 and 700°C respectively [28]. After adsorption, each spectrum has two endothermic peaks located around 48.1 and 116°C, these peaks are related to the evaporation of free water and interstitial water contained in NC after adsorption. The peak at 696°C was assigned to the decomposition of calcite, the endothermic news peaks appears at 518 and 558°C were attributed to the decomposition of methylene blue from NC.



**Figure 4:** DSC of NC before (a) and after (b) adsorption of methylene blue

### *SEM analysis and Optical microscope*

SEM analysis was carried out to evaluate surface morphology of the NC the results are depicted in Figure 5(a). As shown, The SEM image of the NC showed platelet morphology with irregular rough structure. Optical microscopes of NC after and before adsorption the MB are show in Figure 5(b-c). The difference between Figure 5(b) and (c) is clear; there is good possibility that the NC well adsorb the MB.



**Figure 5:** SEM images of NC (a), the pore structure of NC before (b) and after (c) adsorption by optical microscope

### **Adsorption tests**

#### *Effect of Solution pH and point of zero charge (pH<sub>pzc</sub>)*

Adsorption is highly affected by the solution pH, since it change the surface charge on the adsorbent and the adsorbate leading to influences the electrostatic interactions between them [29,30]. The removal of the tested dye by NC at different pH values was studied at initial concentration of 40 mg/L of the dye is presented in Figure 6.a. When the pH was increased from 2 to 12 the adsorption of MB increased from 94.83 to 99.45 %. The result indicated that the dye removal rate is generally influenced by the pH changes and the percentage of MB removal increases with increasing pH of the solution. For a better illustration of these results, it is required to determine experimentally the point of zero charge (pH<sub>pzc</sub>). The point of zero charge of NC was determined as described by the solid addition method using KNO<sub>3</sub> (0.01 M) solution [31]. Initial pH of (0.01M) KNO<sub>3</sub> solutions (pH<sub>i</sub>) was adjusted from pH 2 to 12 by adding either (0.01 M) HCl or 0.01 M (NaOH). Adsorbent dose 0.1g was added to 100 mL of 0.01M KNO<sub>3</sub> solution in 100 mL conical flasks and stirred for 24 h of contact time and final pH (pH<sub>f</sub>) of solution was measured. The difference between the initial and final pH (pH<sub>i</sub>-pH<sub>f</sub>) was plotted against the initial pH (pH<sub>i</sub>) and the point where pH<sub>i</sub>-pH<sub>f</sub>=0 was

taken as the  $pH_{pzc}$ . The results obtained are shown in Figure 6.b. The  $pH_{pzc}$  of NC determined to be 7.6. At a solution of  $pH < 7.6$  the surface becomes positively charged and  $pH > 7.6$  the NC surface is negatively charged. In acid solution the concentrations of  $H^+$  were high and they compete with MB cations for vacant system adsorption sites causing a decrease in dye uptake. The pH of the system increases and  $H^+$  ion concentration decreases, the number of the negatively charged sites increase and the number of the positively charged sites decrease. In this work, all removal tests on NC were affected at normal pH of the solution (without correction) to avoid a possible effect of pH.

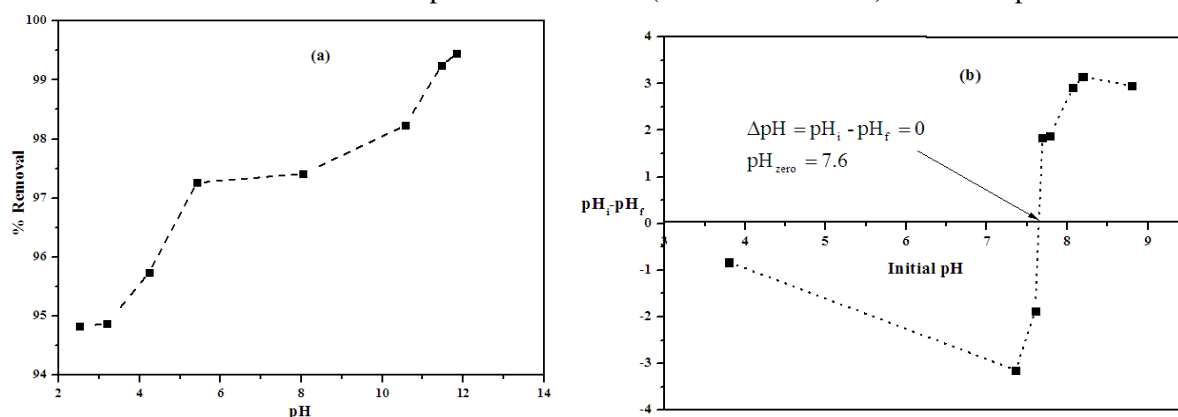


**Figure 6:** Effect of pH on the removal of MB onto NC (a) and determination of the point of zero charge ( $pH_{pzc}$ ) (b)

#### Effect of contact time

The adsorbed quantity and the variation of percentage removal of dye with contact time at different initial concentrations from 14 to 40 mg/L at 25°C and initial  $pH = 6.4 \pm 2$  of natural clay are illustrate in Figure 7 and 8. The maximum adsorptions of BM dye onto NC are 12, 18.4 and 37.8 mg/g at 14mg/L, 20 mg/L and 40mg/L respectively. The removal of MB by adsorption on the adsorbent was shown to increase with time and attained a maximum value at about 120 min and adsorption equilibrium time was 2 h, and thereafter, it remained almost constant. It was clear that the removal of the dye was dependent on the initial concentration of the dye because the increase in the initial dye concentration increased the amount of dye adsorbed. For a contact time of 120 min, percentage dye removal was 72 % for 14 mg/L dye solution, 82% for 20 mg/L dye solution and 92% for 40 mg/L dye solution.

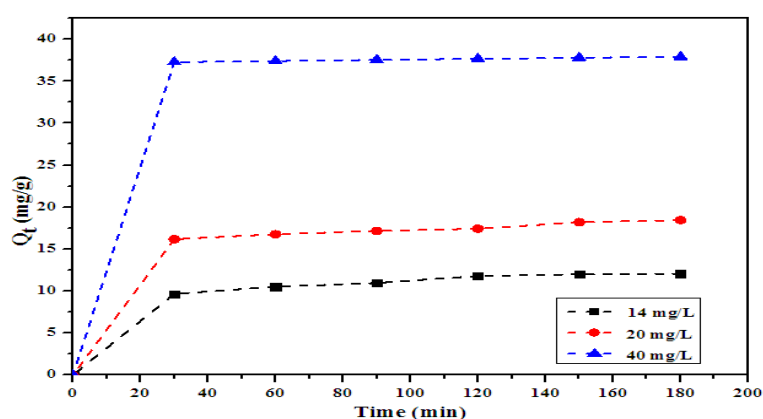


**Figure 7:** Effect of initial dye concentration on adsorption of BM onto NC (dosage 0.1 g,  $pH = 6.4$ ,  $T = 25^\circ C$ , Agitation: 250 rpm)

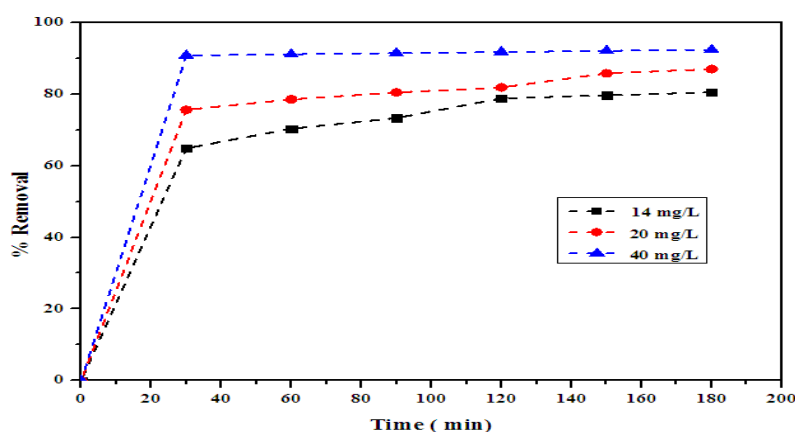


**Figure 8:** Variation of percent of adsorption with adsorption time and with various initial dyes concentrations (dosage 0.1 g, pH = 6.4, T=25 °C, Agitation: 250 rpm)

### *Effect of initial concentration*

The adsorption capacity of NC was examined with the different initial concentration for MB dye. The dye concentration was varied from 10 to 40 mg/L of dye while other experimental parameters; adsorbent ratio (1g/L, pH (5) and contact time (60 min) were kept constant. Figure 9 showed that with the adsorption capacity was observed to be increased with increase in initial concentration of MB using NC. At equilibrium, MB adsorption increased from 9.88 to 23.5 mg/g, with increase in the initial MB concentration from 10 to 40 mg/L. This was because when the initial concentration increased, the mass transfer driving force would become larger, hence resulting in higher MB adsorption [32]. Similar trend was obtained in the adsorption of MB on fly ash [33] and sulfonic acid group modified MIL-101 [34].

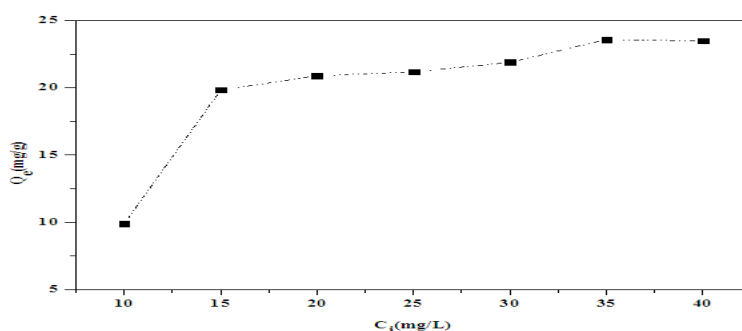


**Figure 9:** Effect of initial MB concentration on the adsorption onto NC.

### *Adsorption Isotherm*

Adsorption is basically important to describe the adsorption mechanisms [35]. Adsorption isotherms are used to determine the adsorption capacity of adsorbent onto adsorbate and understanding behavior to identify the most appropriate adsorption isotherm model. Four famous isotherm equations, Langmuir, Freundlich, Temkin and Dubinin-Radushkevich, were employed for further interpretation of the obtained adsorption data.

### *Langmuir model*

The Langmuir adsorption model [36] is the best known linear template for monolayer adsorption on the homogeneous surface and is used to determine the adsorption parameters. A mathematical expression of the Langmuir isotherm is given by the following equation:



$$\frac{C_e}{q_e} = \frac{1}{K_L q_m} + \frac{C_e}{q_m} \quad (3)$$

Where  $q_e$  (mg/g) is the adsorbed amount at equilibrium,  $C_e$  is the equilibrium dye concentration (mg/L),  $K_L$  is Langmuir equilibrium constant (L.mg<sup>-1</sup>) and  $q_m$  the maximum adsorption capacity (mg/g). The essential characteristics of the Langmuir isotherm can be expressed in terms of dimension less constant separation factor  $R_L$  that is given by the following equation:

$$R_L = \frac{1}{1 + K_L C_0} \quad (4)$$

Where  $C_0$  (mg/L) is the initial concentration and  $K_L$  is the Langmuir constant related to the energy of adsorption (L.mg<sup>-1</sup>). There are four probabilities for the  $R_L$  value: for favorable sorption,  $0 < R_L < 1$ ; for unfavorable sorption,  $R_L > 1$ ; for linear sorption,  $R_L = 1$ ; for irreversible sorption,  $R_L = 0$  [37].

### **Freundlich model**

The Freundlich isotherm [38] is the earliest known relationship describing the adsorption. The equation is conveniently used in the linear form as:

$$q_e = K_F C_e^{1/n} \quad (5)$$

A linear form of this expression is:

$$\ln q_e = \ln K_F + \frac{1}{n} \ln C_e \quad (6)$$

Where  $K_F$  (mg<sup>(1-n)</sup>L<sup>n</sup>g<sup>-1</sup>) is the Freundlich constant and  $n$  (g/L) is the heterogeneity factor. The  $K_F$  value is related to the adsorption capacity; while  $1/n$  value is related to the adsorption intensity.

### **Temkin model**

The Temkin isotherm has been used in the following form [39].

$$q_e = B_T \ln A_T + B_T \ln C_e \quad (7)$$

Where  $B_T = RT/b_T$ ,  $b_T$  is the Temkin constant related to heat of sorption (J/mol),  $A_T$  is the Temkin isotherm constant (L/g),  $R$  is the gas constant (8.314 J/mol K), and  $T$  is the absolute temperature (K).

### **Dubinin-Radushkevich (D-R) model**

Dubinin–Radushkevich (D–R) isotherm is used to distinguish whether the adsorption occurred by physical or chemical processes. The linear form of the isotherm can be expressed as follows [40].

$$\ln q_e = \ln(Q_m) - K\varepsilon^2 \quad (8)$$

where  $K$  is constant related to the adsorption constant (mol<sup>2</sup>/kJ<sup>2</sup>), and  $\varepsilon$  is the Polanyi potential that can be calculated from the equation :

$$\varepsilon = RT \ln\left(1 + \frac{1}{C_e}\right) \quad (9)$$

Where  $R$  is the Universal gas constant (8.314 J.mol<sup>-1</sup> K<sup>-1</sup>),  $T$  (K) is the temperature and  $C_e$ (mg/L) is the equilibrium concentration of MB left in solution.  $q_m$  is the theoretical saturation capacity.

The mean energy of sorption,  $E$  (kJ/mol), is calculated by the following equation:



$$E = \frac{1}{\sqrt{(2K)}} \quad (10)$$

The magnitude of  $E$  is useful for estimating the mechanism of the adsorption reaction. In the case of  $E < 8$  KJ/mol, physical forces may affect the adsorption. If  $E$  is in the range of 8-16 KJ/mol, adsorption is governed by ion exchange mechanism while for the value of  $E > 16$  KJ/mol, adsorption may be dominated by particle diffusion [41, 42].

The results of isotherm parameters are presented in Table 2. The results show that the value of ( $R^2$ ) obtained from Langmuir isotherm equation (0.993) was higher than that from Freundlich (0.511), Dubinin–Radushkevich (0.786) and Temkin (0.59). Comparison of the results for correlation coefficients ( $R^2$ ) indicated that the MB sorption onto natural clay from model solution can be best represented by Langmuir isotherm and adsorption isotherm studies of the MB using NC is an isotherm of the type L in Giles classification [43]. This result indicated that the adsorption process of methylene blue onto the clay was monolayer adsorption, and the maximum monolayer adsorption capacity was found to be 250 mg/g. The  $R_L$  is in the range of 0.53 and 0.9, showing the adsorption of MB on NC is favorable.

**Table 2:** Models isotherm constants for the MB adsorption onto NC

Langmuir				Freundlich			Temkin			Dubinin–Radushkevich		
Q <sub>m</sub>	K <sub>L</sub>	R <sub>L</sub> <sup>2</sup>	Range R <sub>L</sub>	K <sub>F</sub>	1/n	R <sub>F</sub> <sup>2</sup>	A <sub>T</sub>	B <sub>T</sub>	R <sub>T</sub> <sup>2</sup>	Q <sub>m</sub>	R <sub>D-L</sub> <sup>2</sup>	E
(mg/g)	(L/mg)			(mg <sup>1-1/n</sup> /L <sup>1/n/g</sup> )			(L/g)			(mg/g)		(KJ/mol)
25	1.143	0.993	0.08-0.02	14.34	0.203	0.511	85.82	3.378	0.59	24.02	0.786	1.29

### Adsorption kinetic

Kinetics gives important information for designing batch adsorption systems. Information on the kinetics of solute uptake is required for selecting optimum operating conditions for full-scale batch process [44]. Several adsorption kinetics models have been established to describe the adsorption kinetics and the rate-limiting step of the process. In this study, four models were applied to describe the mechanism the adsorption kinetics: the pseudo-first-order, the pseudo-second-order, elovich and intra-particle diffusion.

### Pseudo-first-order model

The pseudo-first order kinetic model of Lagergren was used in order to estimate the adsorption capacity of the adsorbent [45]:

$$\ln(q_e - q_t) = \ln q_e - k_1 t \quad (12)$$

Where  $q_e$  and  $q_t$  are the amounts of dye adsorbed (mg/g) at equilibrium and at time  $t$  (min), respectively, and  $k_1$  (1/min) is the rate constant of pseudo-first-order adsorption.

### Pseudo-second-order model

The pseudo-second-order [46] reaction model is expressed as:

$$\frac{t}{q_t} = \frac{1}{k_2 q_e^2} + \frac{t}{q_e} \quad (13)$$

Where  $q_e$  and  $q_t$  are the amounts of dye adsorbed (mg/g) at equilibrium and at time  $t$  (min), respectively, and  $k_2$  (g/mg.min) is the rate constant of pseudo-second-order adsorption.

### Elovich model

The Elovich equation has been widely used in adsorption kinetics, which describes chemical adsorption (chemical reaction) mechanism in natural [47], the simplified Elovich equation expresses as [48]:

$$q_t = \frac{1}{\beta} \ln(\alpha\beta) + \frac{1}{\beta} \ln t \quad (14)$$

Where  $\alpha$  ( $\text{mg g}^{-1}\text{min}^{-1}$ ) is the initial sorption rate and the parameter  $\beta$  ( $\text{g.mg}^{-1}$ ) is related to the extent of surface coverage and activation energy for chemisorption.

### Intra-particle diffusion

The possibility of intraparticle diffusion was explored by using the intra-particle diffusion model [49]:

$$q_t = k_1 t^{1/2} + I \quad (15)$$

With  $k_1$  is the intraparticle diffusion rate constant ( $\text{mg/g min}^{1/2}$ ) and  $I$  ( $\text{mg/g}$ ) is a constant. The results obtained from the four kinetic models are listed in Table 3. The correlation coefficients ( $R_1^2$ ) for the pseudo first-order kinetic model are between 0.721 and 0.951, the correlation coefficients ( $R_2^2$ ), for the pseudo second order kinetic model are between 0.996 and 1, the correlation coefficients ( $R_3^2$ ) for Elovich model kinetic model are between 0.965 and 0.988 and the correlation coefficients ( $R_4^2$ ) for the Intra-particle diffusion kinetic model are between 0.943 and 0.973, therefore, meaning that that pseudo-second order model best describe the kinetics of the adsorption process. Other part, the values of  $q_e$  calculated from pseudo second order are in good agreement with  $q_e$  experimental values and this indicates that the adsorption system obeys the pseudo second order kinetic model.

**Table 3:** Kinetic constants for MB adsorption onto NC

Dye	Pseudo -first-order				Pseudo-second -order			Intra-particule diffusion model			Elovich		
	$q_{\text{exp}}$	$q_e$	$k_1$	$R_1^2$	$q_e$	$k_2$	$R_2^2$	$I$	$k_{\text{id}}$	$R_3^2$	$\beta$	$\alpha$	$R_4^2$
		(mg/g)	(1/min)		(mg/g)	(g/mg min)		(mg/g)	(mg/g min <sup>0.5</sup> )		(g/mg)		
14 mg/L	12.06	10.51	0.031	0.951	12.34	0.013	0.996	7.891	0.321	0.965	0.7	38.45	0.973
20 mg/L	18.44	9.46	0.023	0.853	18.52	0.013	0.997	14.52	0.286	0.972	0.8	$15 \times 10^3$	0.929
40 mg/L	37.9	7.16	0.031	0.722	38.46	0.052	1	36.80	0.08	0.988	2.88	$4 \times 10^{44}$	0.943

### Thermodynamic parameters

The valuation of temperature was carried out with the scope of testing the ability of NC in MB removal in the case of different temperatures of effluents, dyes tuff wastes. Data were collected at four temperatures from 20 to 60°C. The thermodynamic parameters calculated using the following equations [50]:

$$\Delta G^\circ = -RT \ln K_d \quad (16)$$

$$K_d = \frac{C_a}{C_e} \quad (17)$$

$$\ln K_d = \frac{\Delta S^\circ}{R} - \frac{\Delta H^\circ}{RT} \quad (18)$$

Where  $K_d$  is the distribution constant,  $C_a$  is the amount of dye adsorbed on the natural clay of the solution at equilibrium (mol/L),  $C_e$  is the equilibrium concentration,  $R$  is the gas constant ( $\text{J.mol}^{-1}.\text{K}^{-1}$ ),  $T$  is absolute temperature (K),  $\Delta H^\circ$  is the standard enthalpy,  $\Delta S^\circ$  is the standard entropy and  $\Delta G^\circ$  is the free energy, recorded in Table 4, were obtained from the slope and intercept of a plot of  $\ln K_d$  versus  $1/T$  ( $\text{K}^{-1}$ ). The values of adsorption thermodynamic parameters are listed in Table 4. The negative value of Gibb's free energy ( $\Delta G^\circ$ ) indicated that the adsorption was spontaneous for MB, The negative value of  $\Delta H^\circ$  ( $-12 \text{ KJ.mol}^{-1}$ ) suggests the exothermic nature of adsorption for the NC and the adsorption is physical in nature involving weak forces of attraction[51]. The negative  $\Delta S^\circ$  ( $-29 \text{ KJ.mol}^{-1}.\text{K}^{-1}$ ) value suggests a decrease in the randomness at the solid/solution interface during the adsorption.

**Table 4:** Thermodynamic parameters calculated for the adsorption of MB by the NC

v. Thermodynamic parameters calculated for the adsorption of MB by the NC							
adsorbent	Adsorbate	Thermodynamic parameters					
		$\Delta H^\circ(\text{KJ.mol}^{-1})$	$\Delta S^\circ (\text{KJ.mol}^{-1}.\text{K}^{-1})$	$\Delta G^\circ(\text{KJ.mol}^{-1})$			
				293K	303K	313K	333K
Natural clay	MB	-12	-29	-4.025	-3.053	-2.721	-2.973

#### *Comparison of adsorption capacity with different adsorbent reported in literature*

A comparison of the adsorption capacities MB onto various adsorbents is shown in Table 5. The results obtained experimentally in this study are higher than the results obtained by other investigations. This clearly indicates that the natural clay can be fruitfully used as an adsorbent for cationic dye removal.

**Table 5:** Comparison of monolayer adsorption of MB onto various adsorbents

Adsorbent	Adsorption capacity (mg/g)	References
Raw kaolinite	13.99	[52]
Kaolin	52.76	[53]
diatomite treated with sodium hydroxide	27.86	[54]
Fly ash based geopolymer	37.04	[55]
$\gamma\text{-Fe}_2\text{O}_3$ /acid-activated kaolin	50.2	[56]
montmorillonite clay modified with iron oxide	71.12	[57]
MIL-101(Cr)	22	[58]
Activated charcoal	48.31	[59]
Natural Clay	25	This work

## CONCLUSION

The results that have been obtained in this work can be summarized in the following points:

- Natural clay used is rich in montmorillonite as confirmed by the methods of analysis and chemical composition found in literature.

- The experimental results for solution pH indicate that the percentage of removal increased with increased pH.
- Langmuir model will be the best in description of adsorption isotherm.
- The kinetic at different dye concentrations data tends to fit very well in the pseudo-second-order kinetics model with high correlation coefficients in the case of methylene blue.
- The results of  $\Delta H^\circ$ ,  $\Delta S^\circ$  and  $\Delta G^\circ$  show that the adsorption of methylene blue by natural clay is exothermic and favorable process.
- The results indicate that the natural clay can be used as an efficient and low cost adsorbent for simultaneous removal of dye cationic and the removal of a basic dye at relatively great concentrations in aqueous solution.

## REFERENCES

1. H.D. Setiabudi, R. Jusoh, S.F.R.M. Suhaimi, S.F.Masrur, *Journal of the Taiwan Institute of Chemical Engineers*.(2016)1–8
2. B.H. Hameed, H. Hakimi, *Biochem Eng J.* 39 (2) (2008) 338–43
3. D. Kavitha, C. Namasivayam, *Bioresource Technology.* 98 (2007)14–21.
4. M. A. M. Salleh, D. K. Mahmoud, W. A. W. A. Karim, A. Idris, *Desalination.* 280 (2011)1–13.
5. M.H. El-Naas, S.A. *J. Hazard. Mater.* 164 (2009) 720–725.
6. C. Tocchi, E. Federici, L. Fidati, R. Manzi, V. Vincigurerra, M. Petruccioli. *Water Res.* 46 (2012) 3334–3344
7. Y.Zhang, C. Causserand, P. J.P. Aimar, Cravedi. *Water Res.*40 (2006)3793–3799.
8. A. Dbrowski, Z. Hubicki, P. Podkocielny, E. Robens. *Chemosphere.*56 (2) (2004) 91-106.
9. D.J. Ennigrou, L. Gzara, Ben Romdhane, M.R., Dhahbi. *Desalination.* 246(1-3) (2009) 363-369.
10. B. Mondal, V.C. Srivastava, J.P. Kushawaha, R. Bhatnagar, S. Singh, I.D. Mall. *Sep. Purif. Technol.* 109 (2013)135–143.
11. A.K. Verma, R.R. Dash, P. Brunia. *J. Environ. Manage.* 93 (2012) 154–168.
12. F.A. Banat, B. Al-Bashir, S. Al-Asheh, O. Hayajneh. *Environ. Pollut.*107 (2000) 391-398.
13. R. Elmoubarki, F.Z. Mahjoubi, H. Tounsadi, J. Moustadraf, M. Abdenmouria, A. Zouhri, A. El Albani, N. Barka, *Water Resour. Ind.* 9 (2015) 16.
14. P.T. Hang, G.W. Brindley, *Clays and Clay Minerals.* 18 (1970) 203.
15. H. Amrhar, M. Nassali, S. Elyoubi, *J. Mater. Environ. Sci.* 6 (2015) 3054.
16. A. Denise, Fungaro, C. Lucas, Grosche, S. Alessandro, Pinheiro., Juliana C., Izidoro., Sueli I., Borrelly, J. *Chem. Campo Grande.* 2 (2010) 235.
17. A. Aarfane, A. Salhi, M. El Krati, S. Tahiri, M. Monkade, E.K. Lhadi, M. Bensitel, *J. Mater. Environ. Sci.* 5(2014)1927.
18. A. Aarfane, S. Tahiri, A. Salhi, G. El Kadiri Boutchich, M. Siniti, M. Bensitel, B. Sabour, M. El Krati, *J. Mater. Environ. Sci.*6 (2015) 2944.
19. R. Elmoubarki, F.Z. Mahjoubi, H. Tounsadi, J. Moustadraf, M. Abdenmouria, A. Zouhri, A. El Albani, N. Barka, *Water Resour. Ind.* 9 (2015)16.
20. S.B. Bukallah, M. A. Rauf, S.S. AlAli, *J. Dyes. Pigments.*(2007)74-85.
21. H.H.W. Moenke, Silica, the three-dimensional silicates, borosilicates, and beryllium silicates, in: V.C. Farmer (Ed.), *The Infrared Spectra of Minerals*, Mineralogical Society, London. (1974)365–382.
22. G.C. Yong, H. Yong, Y. Wei-Min, J. Ling-Yan, *Journal of Industrial and Engineering Chemistry.* 2014.<http://dx.doi.org/sci-hub.cc/10.1016/j.jiec.2014.12.006>
23. O.V. Ovchinnikov, A. V. Evtukhova, T.S. Kondratenko, M.S. Smirnov, V.Yu. Khokhlov, O.V. Erina, *Vib. Spec.*2016. <http://dx.doi.org/10.1016/j.vibspec.2016.06.016>
24. R. Mazeikiene, G. Niaura, O. Eicher-Lorka, A. Malinauskas, *Vib. Spectrosc.*, 2008 47, 105-112.
25. S.H. De Araujo Nicolai, P.R. Rodrigues, S.M.L. Agostinho, J.C. Rubim, *J. Electroanal. Chem.* 527 (2002) 103-111.

26. P.H.B. Aoki, D. Volpati, W. Caetano, C. Constantino, *Vib. Spectrosc.* 54 (2010) 93-102.
27. H.H. Freedman, *J. Am. Chem. Soc.* 83 (1961) 2900-2905.
28. Z. Ding, R.L. Frost, *Thermochim. Acta.* 389 (2002) 185-193.
29. N. Barka, S. Qourzal, A. Assabbane, A. Nounah, Y. Aît-Ichou, *J. Saudi Chem. Soc.* 15 (2011) 263.
30. N. Barka, A. Assabbane, A. Nounah, L. Laanab, Y. Aît-Ichou, *Desalination.* (2009) 235-264.
31. ID. Mall, VC. Srivastava, GVA. Kamur, IM. Mishra, *Colloids and Surfaces A: Physicochem. Eng. Aspects*, 278 (2006) 175-187.
32. B.H. Hameed, *J. Hazard. Mater.* 166 (2009) 233-238.
33. V.V. Basava Rao, S. Ram Mohan Rao, *Chem. Eng. J.* 116 (2006) 77-84.
34. X.P. Luo, S.Y. Fu, Y.M. Du, J.Z. B. Guo, Li, *Microporous Mesoporous Mater.* 2016, doi: 10.1016/j.micromeso.2016.09.032.
35. S. Khorshidi, H. Nourmoradi, O. Rahmanian, F. M. Moghadam, S. Norouzi, M. Heidara, *Der Pharma Chemica.* (8) (2016) 233-242.
36. I. Langmuir, *J. Am. Chem. Soc.* 40 (1918) 1361.
37. Sivaraj R., Namasivayam C., Kadirvelu K, *Waste Management*, 21 (2001) 105.
38. H. Freundlich, *J. Z Phys. Chem.* 57 (1906) 385.
39. Temkin M, I, *Zh. Fiz. Chim.* 15 (1941) 296.
40. M.M. Dubinin, E.D. Zaverina, L.V. Radushkevich, *J. Phy. Chem.* 21 (1947) 1351-1362.
41. A.S. Ozcan, B. Erdem, A. Ozcan, *Colloids Surfaces A: Physicochem. Eng. Aspects.* 266 (2005) 73.
42. A. Ozcan, E.M. Oncu, A.S. Ozcan, *Colloids Surfaces A: Physicochem. Eng. Aspects.* 277 (2006) 90.
43. N. Barka, M. Abdennouri, M. EL Makhfouk, *J. Taiwan Inst. Chem. Eng.* 42, 320.
44. Guo. Shenghui, Li. Wei, Z. Libo, P. Jinhui, X. Hongying, Z. Shiming, *Process Safety and Environmental Protection.* 87 (2009) 343-351.
45. S. Lagergren, *Kungliga Svenska Vetenskapsakademiens Handlingar.* 24 (1898) 1-39.
46. Y.S. Ho, G. McKay, *Process. Biochem.* 34 (1999) 451-465.
47. M.I. Temkin, *Zh. Fiz. Chim.* 15 (1941) 296-332.
48. W.J. Weber Jr, J.C. Morris, *J. Sanitary Eng. Div, ASCE.* 89 (1963) 31.
49. VK. Gupta, I. Ali, *J. Colloid Interf. Sci.* 8 (2004) 271.
50. A. Ashraf, El-Bindary, Z. Adel, El-Sonbati, A. Ahmad, Al-Sarawy, S, Khaled. Mohamed, A. Mansour. Farid, *J. Mater. Environ, Sci.* 6 (2015) 1.
51. Ozkan Demirbas, Yasemin Turhan, Mahir Alkan, *Desalin. Water Treat.* (2014) 1-8
52. D. Ghosh, K.G. Bhattacharyya, *Appl. Clay Sci.* 20 (2002) 295-300.
53. W. Gao, S. Zhao, H. Wu, W. Deligeer, S. Asuha, *Appl. Clay Sci.* 126 (2016) 98.
54. J. Zhang, Q. Ping, M. Niu, H. Shi, Li Na, *Appl. Clay Sci.* 83-84 (2013) 12.
55. M. EL Alouani, S. Alehyen, M. EL Achouri, M. Taibi. *J. Mater. Environ. Sci.* 9 (1) (2018) 32-46
56. Z. Gao, X. Li, H. Wu, S. Zhao, W. Deligeer, S. Asuha, *Microporous Mesoporous Mater.* 202 (2015) 1-7.
57. L. Cottet, C.A.P. Almeida, N. Naidek, M.F. Viante, M.C. Lopes, N.A. Debacher, *Appl. Clay Sci.* 95 (2014) 25-3.
58. T. Shen, J. Luo, S. Zhang, X. Luo, *J. Environ. Chem. Eng.* 3 (2015) 1372-1383.
59. E. M. Khan, K. M. Doke, K. B. Thombal, *Der Pharma Chemica.* 3(1) (2011) 306-317